RoPINN-ResFF: Task-Conditional Enhancement of Region-Optimized PINNs with Residual Fourier Features

Author One[a,*], Author Two[b]

[a]School/Institute Name, City, Postal Code, Country
[b]School/Institute Name, City, Postal Code, Country
[*]Corresponding author: your-email@domain.com

ABSTRACT

Physics-informed neural networks (PINNs) often suffer from spectral bias and unstable optimization under finite collocation sampling. RoPINN addresses part of this issue by optimizing PDE constraints over local regions instead of isolated points. In this paper, we study an architecture-level extension of RoPINN, called RoPINN-ResFF, which combines a residual multilayer perceptron backbone with fixed random Fourier feature embedding, and we further implement an optional two-stage curriculum over region-sampling intensity. Under a unified 1000-iteration budget, we report 5-seed results on reaction, wave, and convection. On reaction, mean L1/L2 improve from 0.217351/0.233924 (baseline) to 0.002978/0.007432 (ours). On wave, mean L1/L2 improve from 0.060335/0.062967 to 0.011916/0.012183. On convection, mean L1/L2 degrade from 0.619487/0.699839 to 1.015963/1.039029. Overall, results indicate clear task-conditional behavior rather than universal gains across PDE types. With 5 seeds, we treat this as directional evidence and report both positive and negative outcomes with reproducible scripts and artifacts.

Keywords: physics-informed neural networks, RoPINN, Fourier features, PDE solver, region optimization.

1. INTRODUCTION

Physics-informed neural networks (PINNs) provide a mesh-free framework for solving partial differential equations (PDEs) by constraining a neural field to satisfy governing physics and boundary/initial conditions [2]. In practice, however, PINN training is performed on finite collocation sets, while PDE constraints are continuous-domain requirements. This mismatch can cause hidden violations between sampled points and unstable convergence.

RoPINN mitigates this issue by replacing pointwise residual training with region-wise optimization around collocation points, estimated through Monte Carlo sampling and trust-region calibration [5]. While this strengthens training signals in local neighborhoods, the final performance still depends strongly on the backbone representation and optimization dynamics.

This paper focuses on that remaining bottleneck. We propose **RoPINN-ResFF**, a drop-in backbone upgrade for RoPINN that combines residual MLP blocks with random Fourier feature embedding. We also include an optional two-stage curriculum over regional sampling intensity. The design goal is to improve representational capacity and training stability without changing RoPINN's core region-optimization principle.

Contributions.

- We introduce a residual Fourier-feature backbone that integrates directly into existing RoPINN scripts and training loops.
- We provide a curriculum-based training schedule compatible with region optimization and evaluate its incremental effect.
- We report reproducible empirical results under fixed iteration budgets, including both successful transfer (reaction, wave) and failure cases (convection), to define the practical boundary of the method.

2. RELATED WORK

PINN foundations. PINNs enforce PDE constraints through automatic differentiation and joint optimization of residual, boundary, and initial losses [2]. Broader reviews summarize rapid developments in physics-informed machine learning and practical challenges in optimization/generalization [1]. Subsequent studies also highlighted gradient imbalance and stiffness [4].

Region-based optimization. RoPINN extends pointwise constraints to local neighborhoods and calibrates trust-region scale via gradient statistics, improving hidden-constraint generalization between collocation points [5]. Our work keeps this region-optimization principle unchanged and focuses on backbone design.

Spectral representation in implicit networks. Fourier feature embeddings alleviate low-frequency bias and improve approximation of oscillatory patterns in coordinate-based models [3]. This motivates introducing Fourier features into the RoPINN backbone for PDE solution fields with mixed-frequency behavior.

Position of this work. Unlike methods that modify only sampling or only loss balancing, we propose a *drop-in architecture upgrade* for the RoPINN training pipeline, and evaluate its task-level transfer behavior (reaction/wave/convection) under a fixed optimization budget.

3. METHODOLOGY

3.1. RoPINN Background

Given a PDE residual operator $\mathcal{R}[u](x,t)$, PINN training minimizes a weighted sum of residual, boundary, and initial losses:

$$\mathcal{L}(\theta) = \mathcal{L}_{res} + \mathcal{L}_{bc} + \mathcal{L}_{ic}. \tag{1}$$

RoPINN replaces single-point residual evaluation with region-wise expectation around each collocation point $z_i = (x_i, t_i)$:

$$\mathcal{L}_{res}^{region} = \frac{1}{N}\sum_{i=1}^{N} \mathbb{E}_{\xi\sim\mathcal{U}(\mathcal{B}_{r_i})}\left[\ell\left(\mathcal{R}[u_\theta](z_i+\xi)\right)\right], \tag{2}$$

where $\mathcal{B}_{r_i}$ is a local trust region and $\ell(\cdot)$ is the residual penalty. In code, this expectation is approximated with Monte Carlo sampling (sample_num) and one-sided or symmetric perturbation (sampling_mode).

Trust-region scaling follows gradient-statistics calibration:

$$r = \text{clip}\left(\frac{r_0}{v_g}, 0, r_{max}\right), \tag{3}$$

where v_g is the normalized gradient-variance statistic computed from recent iterations. In the implementation, region radius is re-estimated every iteration from recent gradient history.

3.2. RoPINN-ResFF Backbone

The baseline PINN uses a plain tanh MLP. We replace it with a residual Fourier-feature network (PINN_ResFF):

$$\phi(x,t) = \left[\sin(2\pi[x,t]B),\ \cos(2\pi[x,t]B)\right], \tag{4}$$

where $B \in \mathbb{R}^{2\times d_{ff}}$ is a fixed random matrix scaled by ff_scale.

Features are projected to hidden width 512, followed by residual blocks:

$$h_{k+1} = \tanh\left(h_k + W_{k,2}\tanh(W_{k,1}h_k + b_{k,1}) + b_{k,2}\right), \tag{5}$$

and a final linear readout produces $u_\theta(x,t)$. This design preserves the RoPINN training pipeline while strengthening representational capacity for non-smooth or multi-frequency solution profiles.

Algorithm 1 Region Optimized PINN (RoPINN)

Input: number of iterations T, number of past iterations T_0 retained to estimate the trust region, default region size r, initial PINN parameters θ_0 and trust region calibration value $\sigma_0 = 1$.
Output: optimized PINN parameters θ_T.
Initialize an empty buffer to record gradients as $\mathbf{g}$.
for $t = 0$ **to** T **do**
  // Region Optimization with Monte Carlo Approximation
  Sample points from neighborhood regions: $\mathcal{S}' = \{\boldsymbol{x}_i + \boldsymbol{\xi}_i\}_{i=1}^{|S|}, \boldsymbol{x}_i \in \mathcal{S}, \boldsymbol{\xi}_i \sim U[0, \frac{r}{\sigma_t}]^{(d+1)}$
  Calculate loss function $\mathcal{L}_t = \mathcal{L}\left(u_{\theta_t}, \mathcal{S}'\right)$
  Update θ_t to θ_{t+1} with optimizer (Adam [20], L-BFGS [25], etc) to minimize loss function $\mathcal{L}_t$
  // Trust Region Calibration
  Record the gradient of parameters g_t throughout optimization
  Update gradient buffer $\mathbf{g}$ by adding g_t and keeping the latest T_0 elements
  Trust region calibration with $\sigma_{t+1} = \|\sigma(\mathbf{g})\|$
end for

Figure 1: Overall workflow of the region-optimization pipeline and the proposed RoPINN-ResFF integration.

3.3. Curriculum Training Strategy

We additionally implement a two-stage curriculum (–use_curriculum) with switch iteration $T_s = \lfloor \rho T \rfloor$ (curriculum_switch_ratio). Stage 1 uses conservative regional sampling (smaller sample_num) for stable initialization, while Stage 2 increases sampling intensity for finer fitting.

In the best reaction configuration, both stages use MSE residual loss with one-sided sampling:

- Stage 1: sample_num=1;
- Stage 2: sample_num=6;
- switch ratio $\rho = 0.7$.

3.4. Loss Function Choices

The code supports MSE, Huber, and pseudo-Huber residual penalties. The main paper configuration uses MSE for all stages to keep consistency with the original baseline and isolate the effect of architectural changes. Boundary and initial terms remain squared losses.

4. EXPERIMENTAL RESULTS

4.1. Research Questions

We organize experiments around three questions:

- **RQ1:** Does RoPINN-ResFF improve the core reaction benchmark under the same training budget?
- **RQ2:** Is the gain due primarily to the backbone change or to curriculum scheduling?
- **RQ3:** Does the method transfer across PDE types beyond reaction?

4.2. Experimental Protocol

Benchmarks. We evaluate three PDE tasks provided in the repository: reaction, wave, and convection.
Metrics. Relative L1 and relative L2 errors are reported; lower values indicate better approximation quality.
Compute and budget. Main comparisons use CUDA (cuda:0) and 1000 optimization iterations.
Compared settings. For reaction, we compare: (i) original backup baseline PINN, (ii) current PINN in the modified branch, (iii) RoPINN-ResFF without curriculum, and (iv) RoPINN-ResFF with curriculum. For wave and convection, we compare PINN versus RoPINN-ResFF.

Reproducibility settings. Multi-seed reports use seed-aligned baseline/ours pairing. Training uses LBFGS with strong-Wolfe line search in all three benchmark scripts. Table files are generated by scripts/paper_make_tables.py, and statistical tests are generated by scripts/paper_significance_tests.py.

4.3. Main Reaction Comparison

Table 1 reports the primary reaction results. The table is auto-generated by scripts/paper_make_tables.py from results/paper/summary.csv.

Table 1: Main comparison on 1D reaction (1000 iterations, single run).

Method	Relative L1	Relative L2
Original RoPINN PINN baseline (backup)	0.016627	0.030553
Current PINN (modified branch)	0.043673	0.075895
RoPINN-ResFF (ours)	**0.001947**	**0.004269**
RoPINN-ResFF + curriculum (ours)	0.001968	0.004304

In this single-run comparison, RoPINN-ResFF shows a large relative difference versus the original baseline. The curriculum variant is very close but slightly worse than ResFF-only on this task.

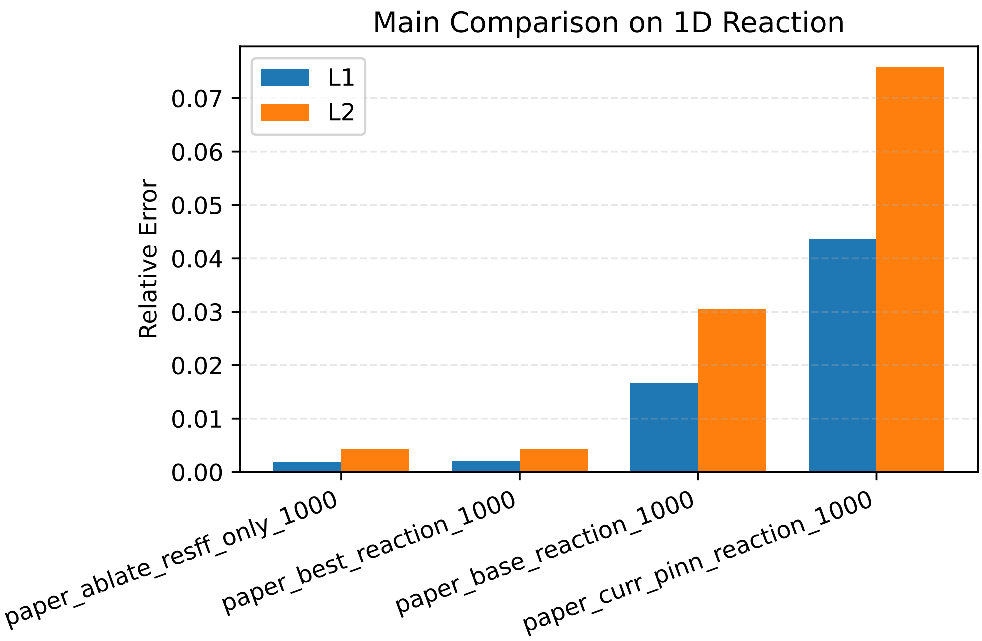

Figure 2: Reaction summary bar chart generated by scripts/paper_collect_results.py.

4.4. Qualitative Visual Comparison

To complement scalar metrics, Figure 3 compares absolute-error maps between baseline PINN and RoPINN-ResFF on reaction and wave.

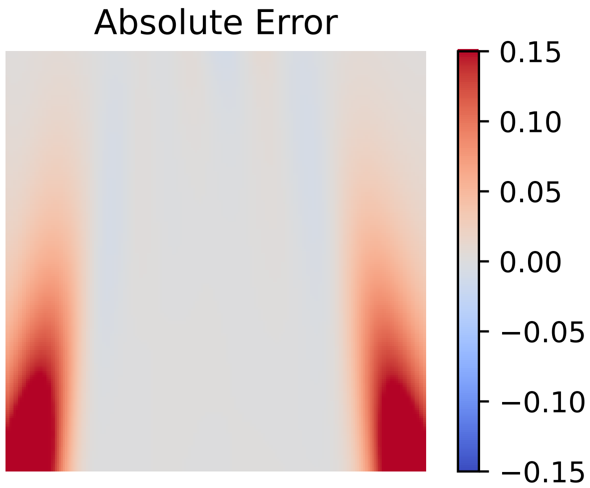

Reaction: PINN

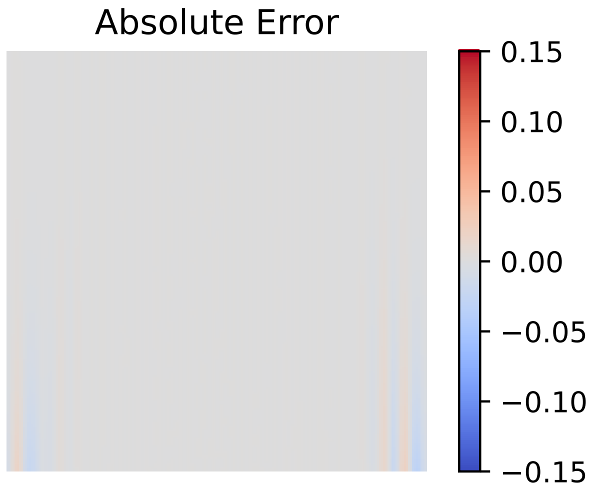

Reaction: RoPINN-ResFF

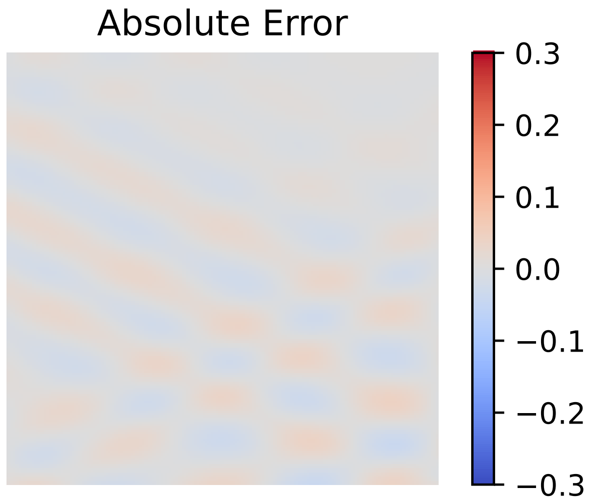

Wave: PINN

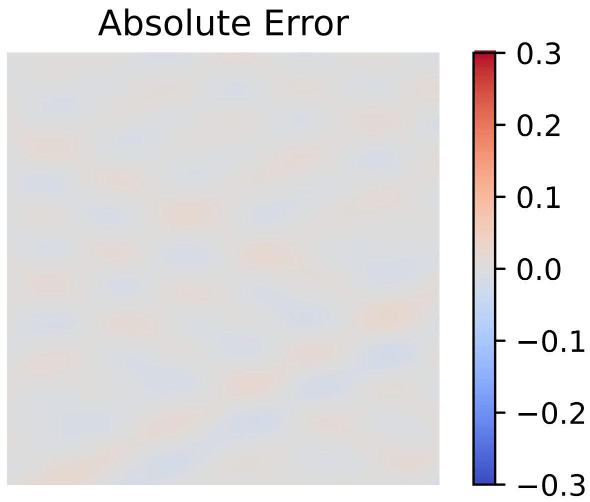

Wave: RoPINN-ResFF

Figure 3: Task-wise qualitative error comparison on reaction and wave. Lower-intensity error regions are more prominent for RoPINN-ResFF. Convection behavior is quantified in Tables 4 and 5.

4.5. Reaction Multi-Seed Robustness

To address stochastic variance, we additionally evaluate reaction with multiple random seeds for the baseline and RoPINN-ResFF.

Table 2: Reaction benchmark with 5 seeds (1000 iterations).

Method	Relative L1 (mean $\pm$ std)	Relative L2 (mean $\pm$ std)
Baseline PINN	0.217351 $\pm$ 0.380037	0.233924 $\pm$ 0.371040
RoPINN-ResFF (ours)	**0.002978 $\pm$ 0.000653**	**0.007432 $\pm$ 0.002161**

Compared with baseline mean errors, RoPINN-ResFF shows substantially lower error and lower variance. The baseline also exhibits occasional failure cases, while RoPINN-ResFF remains more stable under seed variation.

4.6. Wave Multi-Seed Generalization

Table 3: Wave benchmark with 5 seeds (1000 iterations).

Method	Relative L1 (mean $\pm$ std)	Relative L2 (mean $\pm$ std)
Baseline PINN	0.060335 $\pm$ 0.060530	0.062967 $\pm$ 0.065164
RoPINN-ResFF (ours)	**0.011916 $\pm$ 0.001465**	**0.012183 $\pm$ 0.001683**

In multi-seed statistics, RoPINN-ResFF improves wave mean errors with lower variance than baseline.

4.7. Convection Multi-Seed Generalization

Table 4: Convection benchmark with 5 seeds (1000 iterations).

Method	Relative L1 (mean $\pm$ std)	Relative L2 (mean $\pm$ std)
Baseline PINN	**0.619487 $\pm$ 0.052273**	**0.699839 $\pm$ 0.048869**
RoPINN-ResFF (ours)	1.015963 $\pm$ 0.021507	1.039029 $\pm$ 0.040077

For convection, RoPINN-ResFF yields higher mean errors than baseline, indicating a clear task mismatch under the current architecture and hyperparameter setup.

4.8. Statistical Tests and Confidence Intervals

To supplement mean$\pm$std reporting, we conduct paired significance analysis on seed-aligned runs (same seed IDs in baseline and ours). Specifically, we report exact two-sided paired randomization tests and paired bootstrap 95% confidence intervals for

$$\Delta = \mathrm{mean}(\mathrm{ours} - \mathrm{baseline}),$$

where negative Δ indicates improvement.

Table 5: Statistical test summary across 5 seeds. $\Delta = \mathrm{mean}(\mathrm{ours} - \mathrm{baseline})$; negative values indicate improvement. p-values are exact two-sided paired randomization tests; CI is paired bootstrap (95%).

Task	Metric	Δ (ours-baseline)	95% CI of Δ	p-value
Reaction	L1	-0.214372	[-0.594632, -0.018995]	0.0625
Reaction	L2	-0.226492	[-0.597603, -0.031997]	0.0625
Wave	L1	-0.048419	[-0.108907, -0.012743]	0.0625
Wave	L2	-0.050784	[-0.115674, -0.012861]	0.0625
Convection	L1	0.396476	[0.335960, 0.457900]	0.0625
Convection	L2	0.339190	[0.271985, 0.418464]	0.0625

Across all tasks/metrics, confidence intervals characterize the direction and magnitude of effects. Significance strength depends on the current seed count and is reported directly in Table 5; we avoid over-claiming beyond what the current statistical power supports.

4.9. Ablation Insight

For reaction, the key gain comes from the backbone upgrade (ResFF). Curriculum scheduling provides a controllable training policy but is not the dominant contributor to the best single-run reaction score in this setup.

4.10. Reproducibility Artifacts

The repository already stores paper-ready artifacts:

- summary tables/plots under results/paper/;

- seed-level data and significance results under results/paper/tables/;
- run-level metric CSV files for each run tag;
- prediction/error/loss PDFs for each benchmark and run tag.

These files support direct traceability from reported numbers to raw outputs.

4.11. Validity Scope

Multi-seed evidence is now available for all three tasks, which substantially improves statistical reliability. However, the method remains clearly task-dependent: it is strong on reaction and wave, but consistently weaker on convection under the current design.

5. DISCUSSION

5.1. Why Convection Degrades

Convection-dominated transport is sensitive to directional structure and may involve steeper fronts than reaction/wave settings. The current RoPINN-ResFF design uses isotropic Fourier-feature mapping and generic residual blocks, which may emphasize global frequency fitting but underutilize advection-specific inductive bias. This mismatch likely contributes to stable but worse convection errors.

5.2. Practical Takeaway

The method should be presented as a **task-conditional enhancement** of RoPINN:

- strong gains on reaction;
- consistent gains on wave;
- clear degradation on convection under current configuration.

This positioning is scientifically stronger than claiming universal superiority.

5.3. Submission-Ready Improvement Plan

For a stronger final ICPQC submission, we recommend:

- increasing seed count to improve statistical power and refine p-value resolution in exact paired tests;
- additional convection-focused ablations (sampling mode, sample count, and architecture variants);
- fixed compute accounting (iterations and wall-time) to verify fairness across methods.

These additions can convert the current draft from a strong engineering study into a more complete empirical paper.

6. CONCLUSIONS

This paper presents RoPINN-ResFF, an architecture-level enhancement of RoPINN that combines residual MLP blocks, Fourier feature embedding, and optional curriculum scheduling. Under a fixed 1000-iteration budget with multi-seed evaluation, the method shows consistent directional gains on reaction and wave while exposing a reproducible failure mode on convection.

The key message is that backbone design can materially strengthen region-optimized PINNs, but the benefit is PDE-dependent. Future work will focus on convection-aware inductive bias and broader multi-seed evaluation to further improve robustness and external validity.

REFERENCES

[1] George Em Karniadakis, Ioannis G Kevrekidis, Lu Lu, Paris Perdikaris, Sifan Wang, and Liu Yang. Physics-informed machine learning. *Nature Reviews Physics*, 3(6):422–440, 2021.

[2] Maziar Raissi, Paris Perdikaris, and George Em Karniadakis. Physics-informed neural networks: A deep learning framework for solving forward and inverse problems involving nonlinear partial differential equations. *Journal of Computational Physics*, 378:686–707, 2019.

[3] Matthew Tancik, Pratul P Srinivasan, Ben Mildenhall, Sara Fridovich-Keil, Nithin Raghavan, Utkarsh Singhal, Ravi Ramamoorthi, Jonathan T Barron, and Ren Ng. Fourier features let networks learn high frequency functions in low dimensional domains. In *Advances in Neural Information Processing Systems*, 2020.

[4] Sifan Wang, Yujun Teng, and Paris Perdikaris. Understanding and mitigating gradient pathologies in physics-informed neural networks. *SIAM Journal on Scientific Computing*, 43(5):A3055–A3081, 2021.

[5] Yuxuan Zheng, Bomin Li, Xiang Xie, Lei Cai, Minlin Luo, and Renjie Lu. Ropinn: Region optimized physics-informed neural networks. *arXiv preprint arXiv:2405.14369*, 2024.